NJC

Accepted Manuscript

This is an *Accepted Manuscript*, which has been through the Royal Society of Chemistry peer review process and has been accepted for publication.

Accepted Manuscripts are published online shortly after acceptance, before technical editing, formatting and proof reading. Using this free service, authors can make their results available to the community, in citable form, before we publish the edited article. We will replace this *Accepted Manuscript* with the edited and formatted *Advance Article* as soon as it is available.

You can find more information about *Accepted Manuscripts* in the Information for Authors.

Please note that technical editing may introduce minor changes to the text and/or graphics, which may alter content. The journal's standard Terms & Conditions and the Ethical guidelines still apply. In no event shall the Royal Society of Chemistry be held responsible for any errors or omissions in this *Accepted Manuscript* or any consequences arising from the use of any information it contains.

ROYAL SOCIETY OF CHEMISTRY

www.rsc.org/njc

Preparation, characterization and effect of PANI coated TiO_2 nanocomposite on the performance of polysulfone ultrafiltration membranes

Valeen Rashmi Pereira[a], Arun M Isloor[a]*, Amir Al Ahmed[b] and A.F. Ismail[c]

[a]*Membrane Technology Laboratory, Chemistry Department, National Institute of Technology Karnataka, Surathkal, Mangalore 575 025, India*

[b]*Center of Research Excellence in Renewable Energy, King Fahd University of Petroleum and Minerals, Dhahran-31261, Saudi Arabia*

[c]*Advanced Membrane Technology Research Center (AMTEC), Universiti Teknologi Malaysia, 81310 Skudai, Johor Bahru, MALAYSIA*

Abstract

Polysulfone ultrafiltration (UF) membranes with PANI-TiO_2 (Polyaniline-titania) nanocomposite and PEG 1000 (Polyethylene Glycol 1000) as additives were prepared by the phase inversion method. PANI-TiO_2 nanocomposites were synthesized by coating TiO_2 nanotubes with PANI via chemical oxidative polymerization. Synthesized PANI-TiO_2 nanocomposite was characterized by Fourier Transform Infrared Spectroscopy (FTIR), X-ray diffraction (XRD) and Transmission Electron Microscope (TEM) analysis. PANI-TiO_2 nanocomposites with varying concentrations (0 - 1.5 wt %) were dispersed in the polysulfone membrane matrix with N-Methyl-2-pyrrolidone (NMP) as solvent along with PEG 1000 as the pore former. The effect of addition of PANI-TiO_2 nanocomposites with different concentrations (0 - 1.5 wt %) on the membrane structure, performance, hydrophilicity and antifouling nature of the membranes was analyzed. PANI-TiO_2 nanocomposite membranes showed better hydrophilicity, improved permeability, enhanced porosity, water uptake and good antifouling ability when compared with neat polysulfone membranes. The performance of the membranes, improved with the increase in the addition of PANI-TiO_2 nanocomposite. However the membrane performance, decreased slightly at 1.5 weight% addition of PANI-TiO_2 due to the agglomeration of PANI-TiO_2 at higher concentration. The well performed membranes were also subjected to heavy metal ion rejection. The membranes showed rejection of 83.75 % and 73.41 % during Polymer enhanced ultrafiltration (PEUF) process and rejection of 68 % and 53.78 % during the UF process for Pb^{2+} and Cd^{2+} respectively.

Keywords: Polysulfone, PANI-TiO_2 nanocomposite, hydrophilicity

Author for correspondence: E-mail address: isloor@yahoo.com, Fax: 91 824 2474033

1. Introduction

Ultrafiltration is an important membrane separation process which is used for the purification of water,[1] for concentration of solutes and wastewater treatment. Suitable membrane material with good pore structure, permeability, hydrophilicity and antifouling nature plays an important role in the separation process. Polysulfone is one of the widely used materials for the preparation of ultrafiltration membranes,[2] because of its excellent mechanical strength, chemical resistance, thermal stability and good film forming ability.[3] However polysulfone membranes being hydrophobic in nature are susceptible to fouling. Thus the modification of polysulfone membranes is inevitable. Many efforts such as blending hydrophilic additives, chemical grafting, surface coating have been devoted to improve the hydrophilicity of polysulfone membranes.[4] In the recent years, researches have been focused on incorporation of nanomaterials into the membranes to improve the separation performance and fouling resistance.[5] Various inorganic nanomaterials that have been used to improve polysulfone membrane include TiO_2, SiO_2, ZnO, Ag, Al_2O_3, Fe_2O_3. Among these inorganic nanoparticles, TiO_2 has received much attention and is one of the mostly used nanoparticles, due to its stability, availability, antibacterial nature and hydrophilicity.[6]

In the recent years nanohybrid materials with at least two different nanomaterials are gaining interest where the benefits of two different particles could be combined to have improvement in properties.[7] Polyaniline (PANI) based nanocomposites have been extensively studied due its facile preparation and environmental stability.[8] A large number of studies have been focused on preparation of PANI-TiO_2 composites.[9] TiO_2 is considered as the best material to prepare hybrid material with PANI.[10] Ti of TiO_2 has tendency to form co-ordinate bond with N of PANI.[11] PANI-TiO_2 nanocomposites have applications in photocatalysis, charge storage and gas sensors.[9,10] Also polymer/ PANI and PANI/inorganic materials have shown improvement in performance of membranes due to the hydrophilicity of PANI. Teli et al. modified the commercial TiO_2 nanoparticles with PANI and incorporated them into the polysulfone membranes.[11] The obtained membranes had better permeability, higher hydrophilicity and antifouling property. Daraei et al. prepared polyether sulfone nanocomposite membrane with core-shell PANI/Fe_3O_4 nanoparticles which showed enhanced performance for Cu(II) removal from water.[12] Zhao et al. prepared polyaniline−poly(vinylpyrrolidone) (PANI−PVP) nanocomposite and used as an

additive to polysulfone membranes. The membranes showed better permeability and antifouling property.[13]

TiO_2 nanotubes, can act as excellent support materials for PANI, due to their high surface area.[14] On the other hand, TiO_2 nanomaterials are known to undergo agglomeration in order to reduce their surface energy.[15] The presence of PANI on TiO_2 can prevent the agglomeration, increasing the stability of TiO_2 nanomaterials and facilitate uniform dispersion in the polymer matrix. Our previous study indicated that, addition of TiO_2 nanotube has significantly improved the membrane performance.[16] Both PANI and TiO_2 nanotubes have been reported to be good additives in improving the membrane performance.[16,17] The synthesized PANI-TiO_2 nanocomposite could combine the merit of both TiO_2 and PANI and have synergistic effect.[15] Also PANI-TiO_2 having strong interaction between PANI and TiO_2 is known to have well dispersible nature in solvents such as NMP (N-Methyl-2-pyrrolidone).[18] These merits of PANI-TiO_2 are beneficial to the improvement of properties of membrane and hence enhancement in the performance of the membrane is expected.

In this work, PANI-TiO_2 nanocomposites with average diameter of 50 nm were synthesized by coating PANI over TiO_2 nanotubes. PANI coated nanotubes were dispersed in polysulfone membranes containing PEG 1000 as a pore former. The effect of addition of PANI-TiO_2 nanocomposite on the membrane performance, such as permeability, hydrophilicity, porosity and antifouling properties were studied. To the best of our knowledge, it is the first time TiO_2 nanotubes coated with PANI have been used as hydrophilic additives for the performance improvement of polysulfone membranes.

2. Materials and methods

2.1. Materials

`Polysulfone (Psf) with molecular weight 35,000 Da, aniline (99.5%) and TiO_2 nanoparticles were purchased from Sigma Aldrich Co. Bangalore, India. Polyethylene glycol 1000 (PEG 1000) was purchased from Himedia Laboratories Pvt. Ltd., India. Ammonium peroxydisulfate (APS) and Bovine Serum Albumin (BSA) was purchased from Central Drug House (CDH), New Delhi. Hydrochloric acid (HCl), sodium hydroxide (NaOH) and N-Methyl-2-pyrrolidone (NMP) was purchased from Merck India, Ltd. Polyethyleneimine (PEI)

(Mn~60,000) 50 wt% aq. solution, branched was purchased from Acros Organics, USA. Lead (II) nitrate and Cadmium nitrate tetrahydrate and were purchased from Sigma-Aldrich Co, Bangalore, India.

2.2. Preparation of PANI coated TiO_2 nanotubes

TiO_2 Preparation of TiO_2 nanotubes from TiO_2 nanoparticles was done as per the literature.[16] About 50 mL of 10 M NaOH solution was taken in a round bottom flask attached to a condenser with chilling. The solution was first heated to 120^{o}C followed by the addition of 2g of TiO_2 nanoparticles. The solution was then refluxed at the same temperature for 48 h under stirring. Then the mixture was cooled to room temperature and poured into de-ionised water. After the nanotubes were settled at the bottom, the supernatant solution was decanted and was washed repeatedly with water. 150 mL of 0.1 M HCl was then added to the solution and was stirred for 12 hrs at 60^{o}C. Then the nanotubes were again washed with de-ionized water until the neutral pH was obtained. The solution was centrifuged and the obtained nanotubes were calcined at 450^{o}C for 4 h.

Surface modification of the TiO_2 nanotubes by PANI was carried out by chemical oxidative polymerization as follows.[19] 1 mL of aniline was added to 100 mL of 2M HCl solution. 1 g of TiO_2 nanotubes were added to 5 mL of water and sonicated for a few minutes in order to prevent the agglomeration of the TiO_2 nanotubes. This solution was then added to the solution containing aniline and stirred for two hours. The polymerization of aniline was carried out by the addition of ammonium persulfate solution with an equal molar ratio to aniline to the above suspension at room temperature. The product formed was isolated from the dispersion by centrifugation, washed with HCl and water and dried at 80^{o}C for 24 h.

2.2.1. Characterization of PANI coated TiO_2 nanotubes

PANI coated TiO_2 nanotubes were characterized by Fourier Transform Infrared (FTIR) spectroscopy, X-ray diffraction (XRD) and Transmission Electron Microscope (TEM). FTIR spectra were recorded from SHIMADZU ATR-FTIR spectrophotometer. XRD measurements were obtained from Rigaku Miniflex 600 with Cu Kα radiation. Transmission Electron Microscope (JEOL JEM-2100) was used to analyze the morphology of PANI coated TiO_2 nanotubes.

2.3. Preparation of membranes

The nanocomposite membranes were prepared by the phase inversion method. Firstly, PANI coated TiO_2 nanotubes were dispersed in NMP and sonicated for a few minutes for well dispersion. 5 wt% of PEG 1000 was dissolved in NMP and was added as a pore former for all the membranes. 2g of Psf was added to the same dispersion, and was kept for stirring at 60^{o}C for 6 h. After the complete dissolution of Polysulfone, the casting solution was sonicated for 15 min and left still under heating without stirring for 30 min to remove any trapped air bubbles. Then the homogenous solution was casted onto the glass plate. After casting, the glass plate was immersed in a coagulation bath (water) for the phase inversion. The obtained membranes were washed thoroughly with water and dried. The composition of the prepared membranes is given in Table 1.

Table 1 Composition of the membranes

Membranes	**Psf (wt %)**	**PEG (wt %)**	**PANI-TiO_2 (wt %)**	**NMP (wt %)**
P-0	20	5	0	75
P-0.05	20	5	0.05	74.95
P-0.5	20	5	0.5	74.5
P-1.0	20	5	1.0	74
P-1.5	20	5	1.5	73.5

2.3.1. Membrane Characterization

2.3.1.1. Morphology of membranes

The morphology of the prepared membranes was examined using Scanning Electron Microscope (JEOL JSM-6380LA). Before the Scanning Electron Microscope (SEM) analysis, the membranes were dipped and broken in liquid nitrogen and sputtered with gold for conductivity.

2.3.1.2. AFM measurements

The AFM (Atomic Force Microscope) measurements were carried out using Innova SPM Atomic Force Microscope. The measurements were done on dry membrane samples. The

membrane surfaces were imaged in tapping mode. Antimony doped silicon cantilever having force constant in the range of 20-80 N/m was used to analyze the membrane surface topography. The surface roughness of the membranes, expressed in terms of average roughness (Ra) and root mean square roughness (Rq) was measured.

2.3.1.3. Porosity and pore size

The porosity (ε) of the membranes was obtained by gravimetric method.[20]

$$\varepsilon = \frac{w_1 - w_2}{A \times l \times d_w}$$

Where w_1 and w_2 is the weight of the wet and dry membranes respectively. 'A' is the effective membrane area (m^2), 'l' is the thickness of the membrane and 'd_w' is the density of water.

Surface pore size of the membranes in terms of mean pore radius(r_m) was analyzed using Guerout–Elford–Ferry equation,[20] taking into account porosity and water flux of the membranes.

$$r_m = \sqrt{\frac{(2.9 - 1.75\varepsilon) \times 8\eta l Q}{\varepsilon \times A \times \Delta P}}$$

where 'ε' is the porosity, 'η' is the viscosity of water (8.9×10^{-4} Pa s), 'l' is the thickness of the membrane, 'Q' is the volume of pure water permeated through the membrane per unit time (m^3/s), 'A' is the effective membrane area (m^2) and ΔP is the operating pressure (0.2 MPa).

2.3.1.4. Water Uptake Study

In order to study the water uptake capacity of the membranes, membrane samples were cut into 1 cm^2 size and kept immersed in distilled water for 24 h. The wet membranes were weighed immediately after blotting the surface water. The membrane samples were then dried in the vacuum oven at 45°C for few hours. The weight of the dry membrane samples was noted. From the wet and dry weights of the membranes, percent water uptake by the membranes was calculated using the equation

$$\%\ \text{water uptake} = \left(\frac{W_w - W_d}{W_w}\right) \times 100$$

where 'W_w' and 'W_d' are the weights of the wet and dry membranes respectively.

2.3.1.5. Contact Angle Measurement

To evaluate the hydrophilicity of the membranes, the contact angle between water and membrane surface was measured by sessile droplet method using FTA-200 Dynamic contact angle analyzer.[21] In order to minimize the experimental error, for each sample the contact angle was measured at three different locations and the average value was considered.

2.3.1.6. Pure water flux

The permeation properties of the membranes were tested using dead end filtration cell. An effective membrane area of 5 cm^2 was used for permeation studies. The membranes were initially dipped in distilled water for 24 h before the filtration experiments. The membranes were compacted at 0.4 MPa transmembrane pressures (TMP) for 30 min. Then the pressure was reduced to 0.2 MPa, TMP and time dependent pure water flux of the different membranes was measured for every 1 min time interval. The pure water flux (PWF) of the membranes was calculated using the following equation

$$J_{w1} = \frac{Q}{A\,\Delta t}$$

where J_{w1} is the pure water flux expressed in L/m^2h, Q is the quantity of pure water collected (L) in time Δt (h), A is the effective membrane area (m^2).

2.3.1.7. Antifouling study

Bovine Serum Albumin (BSA) was taken as a model protein to study the antifouling nature of the prepared membranes. An aqueous solution of BSA with concentration 0.8g/L was placed in the filtration cell after the pure water flux measurement J_{w1} (L/m^2h).[22] Then the BSA solution was filtered through the membranes for 30 min at 0.2 MPa, TMP. After the BSA filtration, the fouled membranes were washed with pure water for 20 min and then the water flux J_{w2} (L/m^2h) was measured again. In order to estimate the fouling resistant ability of the membranes, flux recovery ratio (FRR) was calculated using the equation

$$\text{FRR}\,(\%) = \frac{J_{w1}}{J_{w2}} \times 100$$

2.3.1.8. Heavy metal ion rejection

Heavy metal ion rejection by the membranes was carried out by polymer enhanced ultrafiltration (PEUF) and ultrafiltration (UF) process. For PEUF process, aqueous solutions of Pb^{2+} and Cd^{2+} were prepared at an initial concentration of 1000 ppm in 1 wt% of the PEI aqueous solution. The pH of the solutions was adjusted to 6.25 by adding small amounts of either 0.1 M HCl or 0.1 M NaOH. Solutions containing the metal ions and PEI were mixed thoroughly and left standing for 5 days for completion of binding between metal ions and PEI. PEI complexed metal ion solutions were filtered through the membranes and the permeate was collected. In UF process, feed solutions containing 1000 ppm of Pb^{2+} and Cd^{2+} were filtered individually through the membranes and the permeate was collected. The % rejection of the metal ions by the membranes during the filtration was determined by analyzing the concentration of feed and permeate solution using Atomic Absorption Spectrophotometer (GBC 932 Plus). Heavy metal ion rejection percentage by the membranes was calculated using the formula

$$\%R = \left(1 - \frac{C_p}{C_f}\right) \times 100$$

where C_p (mg/ml) and C_f (mg/ml) are concentration of metal ions in the permeate and the feed respectively.

3. Results and discussion

3.1. PANI coated TiO_2 nanotubes characteristics

PANI coated TiO_2 nanotubes were prepared via chemical oxidative polymerization.First the synthesised TiO_2 nanotubes were dispersed in HCl solution containing aniline. In the presence of HCl, aniline gets transformed to anilinium cation. Under acidic conditions, the anilinium ions adsorb on the surface of TiO_2 nanotubes and then undergo oxidative polymerization in the presence of ammonium persulfate $(NH_4)_2S_2O_8$, leading to the formation of PANI coating on TiO_2[15].

FTIR spectra of pure TiO_2, pure PANI and PANI-TiO_2 nanocomposite were obtained in the range of 500-3700 cm^{-1}. Fig. 1 shows FTIR spectra. Pure TiO_2 shows broad peak around 3400 cm^{-1} and small peak at 1638 cm^{-1} which is due to the stretching vibration of hydroxyl group (-OH) and adsorbed water present on TiO_2.[23] Broad peak at 600 cm^{-1} ranging from 1000 to 550 cm^{-1} is due to the Ti-O-Ti bonds. FTIR spectrum of PANI shows peak at 1567 cm^{-1} and 1487 cm^{-}

[1] which is due to the C=N and C=C stretching vibrations of quinoid and benzenoid rings of PANI respectively. Further peaks at 1298 cm^{-1} and 1246 cm^{-1} can be ascribed to the C-N stretching mode of benzenoid ring. Peaks at 1141 cm^{-1} and 812 cm^{-1} correspond to the C-H in plane and out of plane bending vibrations respectively.[24] All these peaks of PANI were observed in the IR spectrum of PANI-TiO_2 nanocomposite along with the the broad –OH peak at 3400 cm^{-1} which is observed to surface hydroxyl group of TiO_2. Also the broad peak ranging from 1000 to 550 cm^{-1} due to Ti-O-Ti vibrations was observed in PANI-TiO_2 nanocomposite, indicating the presence of PANI on TiO_2.

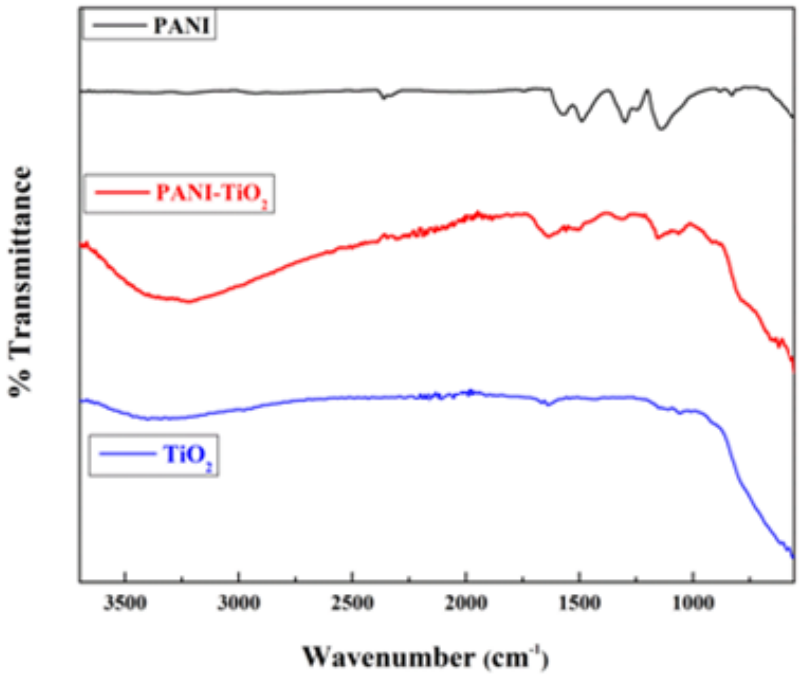

Fig. 1 FTIR spectra of PANI, PANI-TiO_2 nanocomposite and TiO_2

X-Ray diffraction patterns of PANI-TiO_2 nanocomposite, compared with pure PANI and pure TiO_2 are shown in Fig. 2. Pure PANI shows two broad peaks at $2\theta=17^o$ and 23^o which can be ascribed to the (111) and (110) planes. The XRD pattern of pure TiO_2 shows sharp peaks at 25.3^o, 37.8^o, 48.1^o, 54.6^o and 62.6^o with respect to (101), (103), (200), (105) and (213) planes respectively of anatase phase of TiO_2.[10,25] The PANI- TiO_2 nanocomposite showed two broad peaks at $2\theta=17^o$ and 23^o and also all sharp peaks of TiO_2 which confirmed the presence of PANI coating on TiO_2 nanotubes.

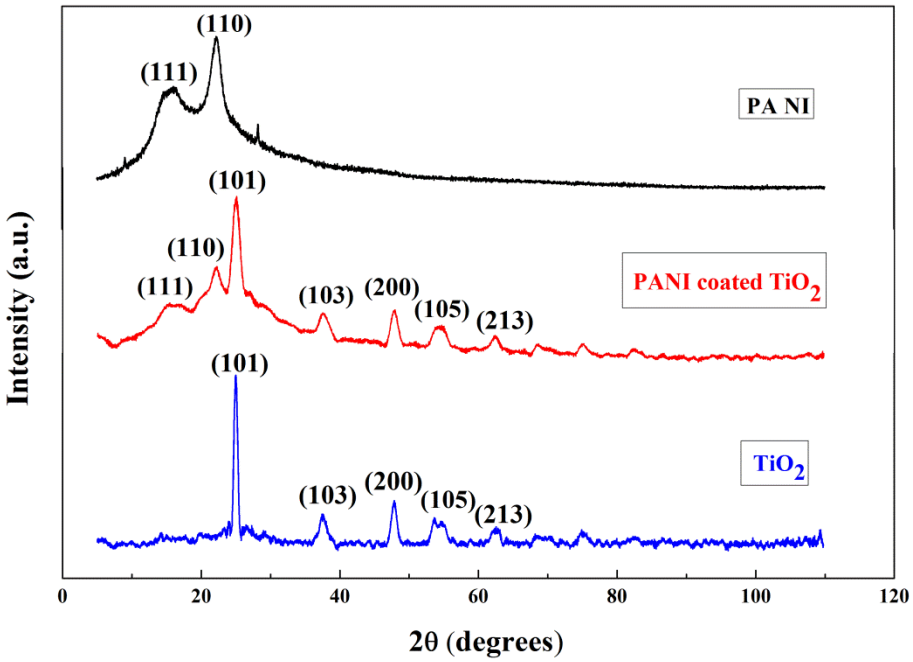

Fig. 2 X-Ray diffraction patterns of pure PANI, PANI-TiO_2 nanocomposite and pure TiO_2

TEM was carried out observe the shape and size of PANI coated TiO_2 nanotubes.TEM images of PANI coated TiO_2 nanotubes are shown in Fig. 3. PANI coated TiO_2 nanotubes had diameter in the range of 40-50 nm.

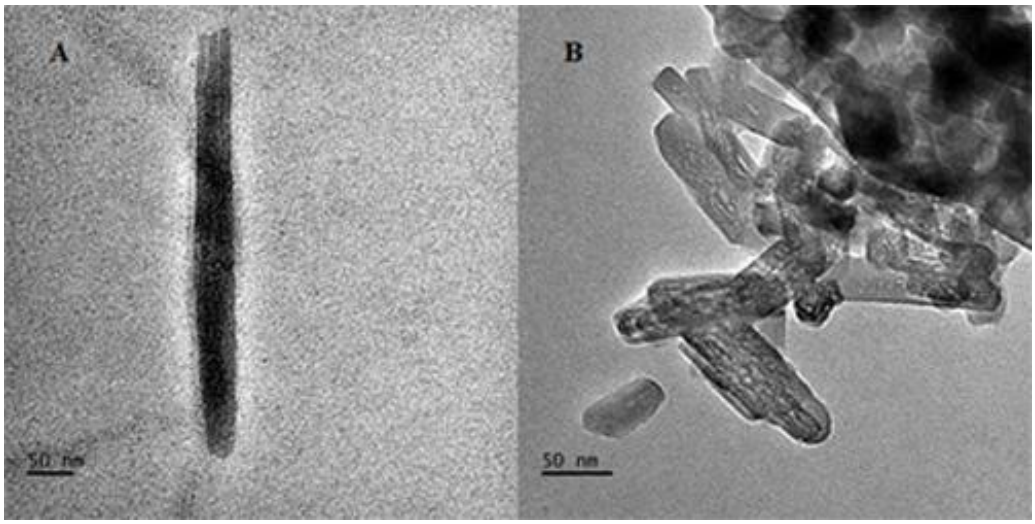

Fig. 3 TEM images of PANI coated TiO_2 nanotubes (A and B)

3.2. Membrane characterization

3.2.1. Membrane morphology

The internal structure and the pore morphology of all the membranes was studied using SEM. Fig. 4 displays the cross-sectional morphologies of the prepared membranes. The cross sectional images show that all the membranes exhibited typical asymmetric structure with dense top layer and porous sub layer. The nanocomposite membranes had well interconnected finger like pores from membrane top layer to sub layer. The addition of PANI-TiO_2 to the membranes brings about change in membrane structure. The finger like pore walls were linked with each other by sponge wall, which allow the finger like pores to communicate with each other. This is due to the well distribution of PANI- TiO_2 nanocomposite in the membranes.[11] The SEM images showed that membrane porosity increased along with pore length as the PANI-TiO_2 content in the membranes increased. Also the skin layer becomes thin and more porous with PANI-TiO_2 content. This is due to the migration behavior of PANI i.e. during membrane formation hydrophilic additive would migrate near the membrane water interface in order to minimize the interfacial energy, thus acting as hydrophilic modifying agent.[13] As a pore former, the addition of PEG would also favor the pore formation. However the effect of PEG on the membrane morphology would be same for all membranes as same amount PEG was added to all the membranes.

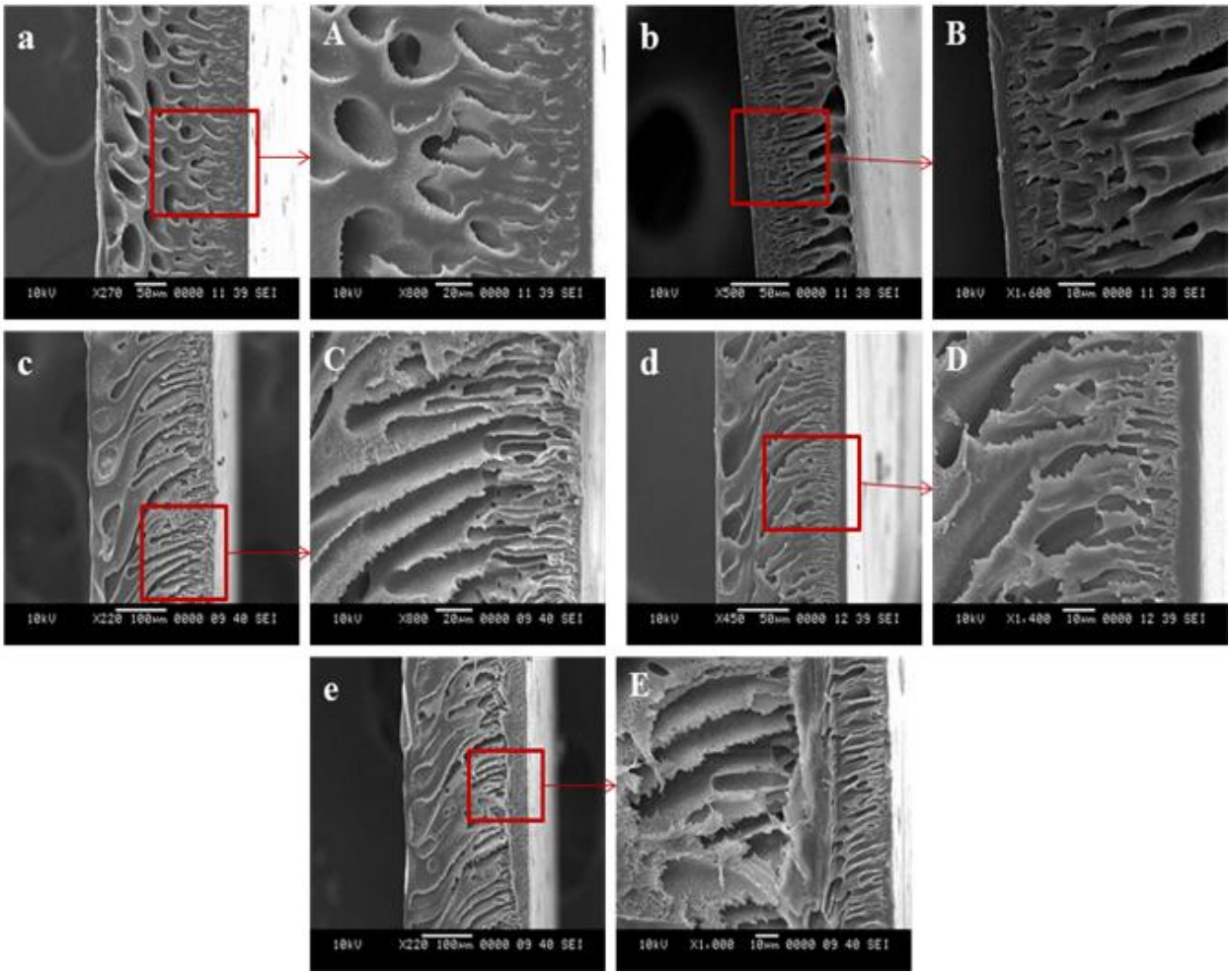

Fig. 4 Cross sectional images of a) P-0 b) P-0.05 c) P-0.5 d) P-1.0 and e) P-1.5 membranes (A, B, C, D and E are the enlarged images of a, b, c, d and e respectively)

3.2.2. Surface topography of membranes

The surface roughness of the membranes were studied using AFM under tapping mode. Fig. 5 shows two-dimensional and three-dimensional scans of P-0, P-0.5 and P-1.0 membranes. From the images, it can be seen that the surface of the membrane P-0 was very rough and the surface roughness reduced for membranes P-0.5 and P-1.0, containing PANI- TiO_2 nanocomposite. The decrease in membrane surface roughness may be due to the uniform dispersion of PANI- TiO_2 in the polymer matrix.[4,12] The decrease in surface roughness of the membranes was confirmed by the surface roughness parameters obtained for P-0, P-0.5 and P-1.0 membranes (Table 2). The mean roughness (R_a) and root mean square roughness (R_q) was

334 and 402 nm for P-0, 54.2 and 67nm for P-0.5 and 41.6 and 51.8 nm for P-1.0 membrane respectively.

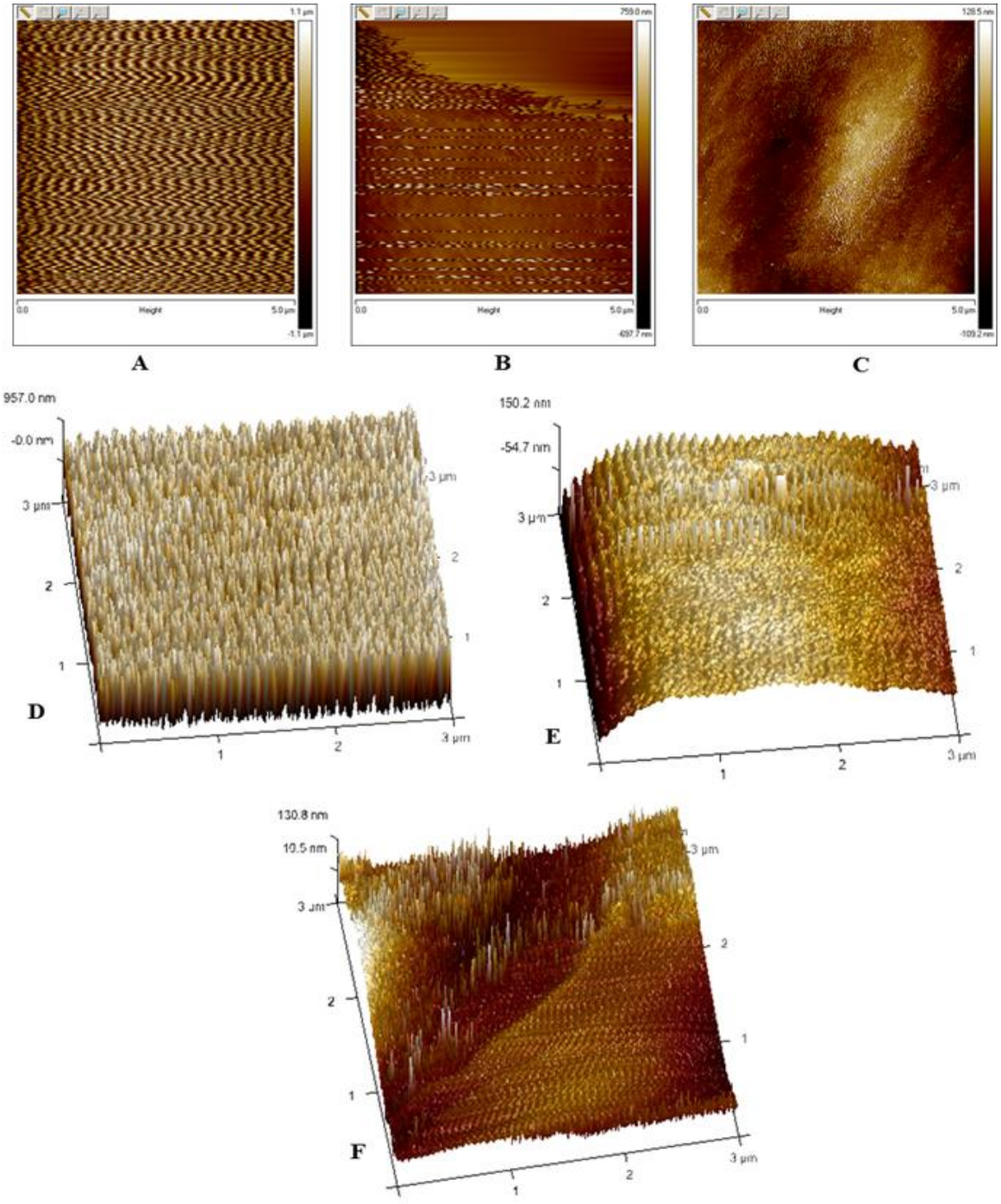

Fig. 5. Two-dimensional scans of A) P-0, B) P-0.5 and C) P-1.0 membranes and three-dimensional scans of D) P-0, E) P-0.5 and F) P-1.0 membranes

Table 2 Surface roughness parameters of membranes

Membranes	Roughness Parameters	
	R_a (nm)	R_q (nm)
P-0	334 ±17.2	402 ±29.0
P-0.5	54.2 ±6.9	67 ±7.1
P-1.0	41.6 ±1.5	51.8 ±4.8

3.2.3. Porosity and pore size of membranes

The surface pore radius and porosity of the membranes are presented in Table 3. The addition of PANI-TiO_2 nanocomposite to the membranes increases the pore size of the membranes except for P-0.5. The higher hydrophilicity of PANI coated TiO_2 nanotubes at higher content would cause an increase of pore size. It is observed that with the initial addition of PANI-TiO_2, the membranes showed a sudden increase in pore size for P-0.05 with 0.05 wt% of PANI-TiO_2 content. The initial increase in pore size may be due to the reason that the addition of nanocomposites to the casting solution increases the thermodynamic instability of the solution, causing rapid demixing, resulting in large pore formation at lower concentration. The low pore radius for P-0.5 membrane is due to the reason that as the addition of PANI-TiO_2 is increased from 0.05 wt% to 0.5 wt%, the viscosity of the casting solution is increased. This delays the exchange of solvent and nonsolvent which results in the suppression of the pore size.[13,26] The membrane with highest PANI-TiO_2 content showed slight reduction of pore size, which might be due to the clogging of pores by the nanocomposite. The clogging of pores at higher concentration of PANI nanocomposite has also been observed in literature.[11] The porosity measurements indicate that the nanocomposite membranes have higher porosity than the pristine membrane. Thus the addition of PANI- TiO_2 has led to the increase in porosity of membranes which is evident from SEM images.

Table 3 Mean pore radii and porosity of membranes

Membranes	**Mean pore radius (nm)**	**Porosity (%)**

P-0	8.25	53.36
P-0.05	14.21	69.60
P-0.5	7.02	76.09
P-1.0	10.72	72.34
P-1.5	8.52	82.60

3.2.4. Water Uptake

Fig. 6 shows the water uptake by the membranes. The least water uptake is shown by membrane P-0 whereas the water uptake of nanocomposite membranes is higher and increases with the increase in PANI-TiO_2 nanocomposite. Water uptake property of the membranes depends on the porosity of the membranes. As the porosity of P-0 membrane is least among all the membranes (Table 3), membrane P-0 showed least water uptake. The increase in water uptake by PANI-TiO_2 nanocomposite membranes with PANI-TiO_2 is due the increasing porosity of the membranes. A slight decrease in water uptake shown by P-1.0 membrane may be due to the less porosity observed for the membrane.

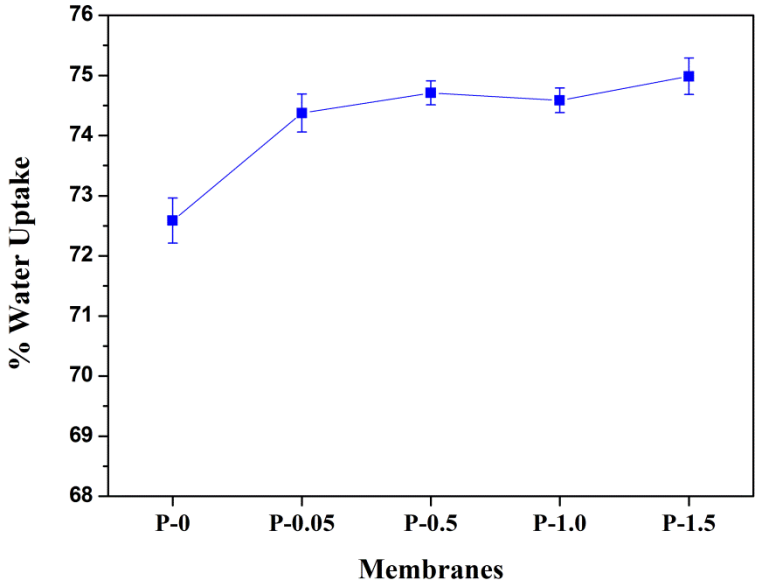

Fig. 6 Water uptake by the membranes

3.2.5. Contact Angle of membrane surfaces

The contact angle of membranes represents the hydrophilicity and wettability of membranes. Fig. 7 shows the contact angle of the membranes. Membrane P-0, showed highest

contact angle indicating its hydrophobic nature. Membrane P-0 did not contain any PANI-TiO_2 nanocomposite and high contact angle is supposed to be due to the hydrophobic nature of polysulfone. The contact angle of PANI-TiO_2 nanocomposite membranes were in the range of 66-64^o. Also the contact angle decreased with the increase of PANI-TiO_2 content in the membranes. The membrane with 1.0 wt % PANI-TiO_2 content showed least contact angle. The decrease in contact angle with the increasing concentration of PANI-TiO_2 in membranes indicated that PANI-TiO_2 nanocomposite enhanced the hydrophilicity of the membranes. Fig. 8 shows the images of contact angle measured on the membranes.

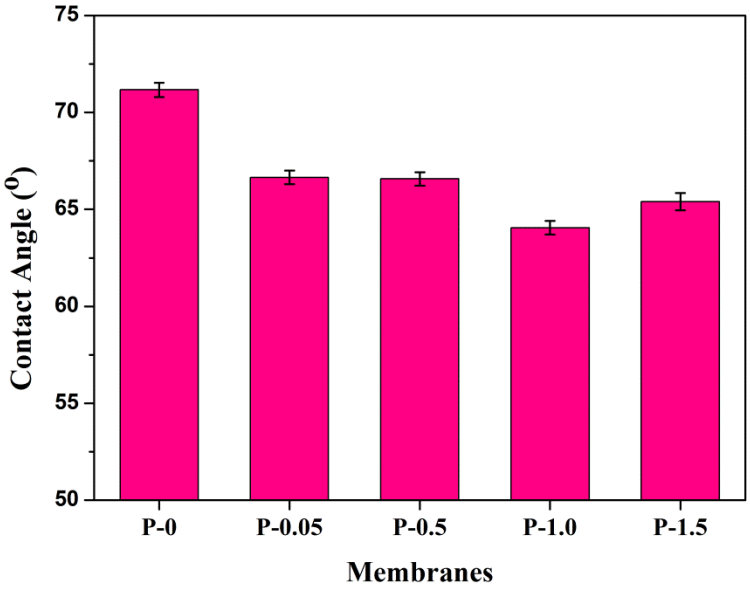

Fig. 7 Contact angle of the membranes

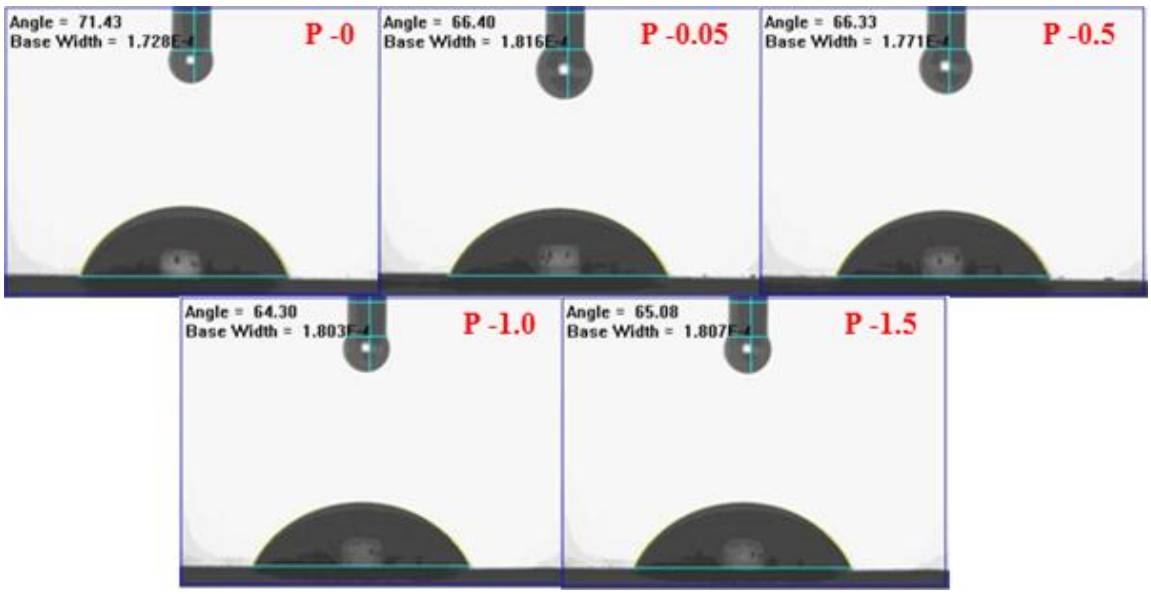

Fig. 8 Images of contact angle measured on the membranes

3.2.6. Permeation properties

Permeation properties of the membranes were studied by permeating pure water through the membranes using dead end filtration cell at 0.2 MPa, TMP. The pure water flux of the membranes is shown in Fig. 9. All the nanocomposite membranes showed higher permeate flux than the polysulfone membrane. The nanocomposite membranes possessed higher hydrophilicity, higher porosity and better vertically interconnected pores than the polysulfone membrane which led to the water permeability of the membranes. The pure water flux of the membranes is in the order P-0<P-0.5<P-1.5<P-0.05<P-1.0. The membranes P-0.05 and P-1.0 showed higher water flux among the synthesized membranes. This is due to the higher pore sizes of these membranes when compared to the other membranes (Table 3). Among P-0.05 and P-1.0 membranes, though the pore radius of P-1.0 was lower than that of P-0.05 membrane, the higher PWF is due to the higher hydrophilic nature of P-1.0 membrane than P-0.05 membrane. The contact angle measurements showed that, membrane P-1.0 possessed highest hydrophilicity. Higher PANI-TiO_2 content, higher would be the hydrophilic nature of PANI and TiO_2 which would attract water molecules easily into the membrane matrix thereby increasing the permeability.[6] Among P-0, P-0.5 and P-1.5 membranes, P-0 showed least PWF due to the reason that membrane P-0 is hydrophobic in nature and did not contain any PANI-TiO_2 nanocomposite. Though the pore radius of P-0.5 was lesser than that of P-0 membrane, the PWF is higher

because of the presence of hydrophilic PANI-TiO_2 and higher porosity of the membrane. Membrane P-1.5 had higher PWF than P-0 and P-0.5 membranes, because its pore size was higher than that of both P-0 and P-0.5 membrane. However the PWF of P-1.5 membrane was lower than that of P-0.05 and P-1.0 membranes, because the presence of excessive PANI-TiO_2 content led to the clogging of pores which in turn decreased the permeability of the membrane. Similar results showing decrease in flux with the increase in concentration of PANI and PAni based nanocomposites in the membranes has been found in literature.[13,24]

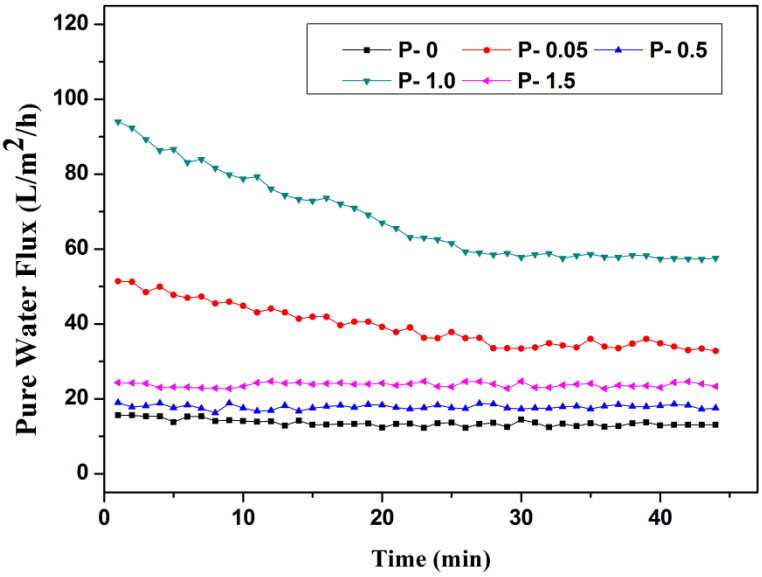

Fig. 9 Pure water flux of the membranes

3.2.7. Antifouling properties

The fouling nature of the membranes was investigated through protein filtration, using BSA as a model protein. The flux of the membranes during BSA filtration is shown in Fig. 10. The figure shows decline in flux of membranes for initial few minutes. This initial decline of flux is due to the adsorption of BSA molecules onto the surface of the membranes.[27] All the membranes showed higher flux than P-0 membrane. Since the nanocomposite membranes had higher hydrophilicity, protein molecules could not be easily adsorbed on the membrane surface indicating antifouling nature of membranes.[13] The % FRR values of the membranes are shown in Fig.11. Higher the FRR value better is the antifouling nature of the membranes.

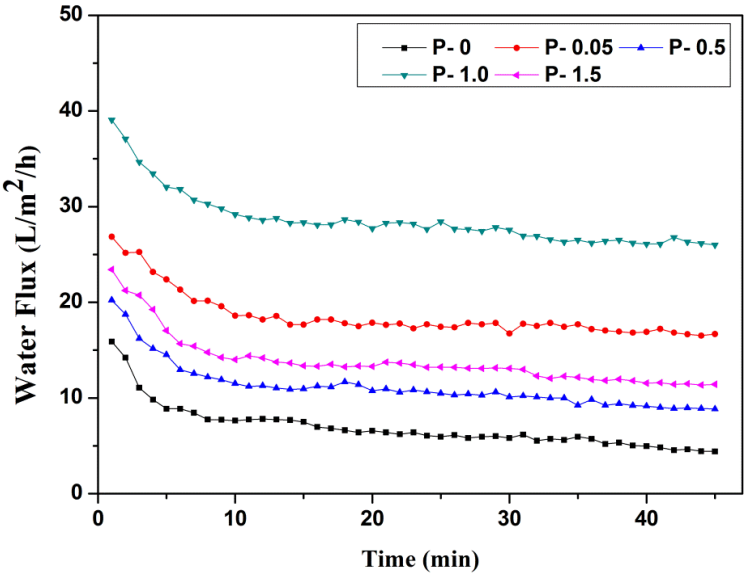

Fig. 10 Flux of the membranes during BSA filtration

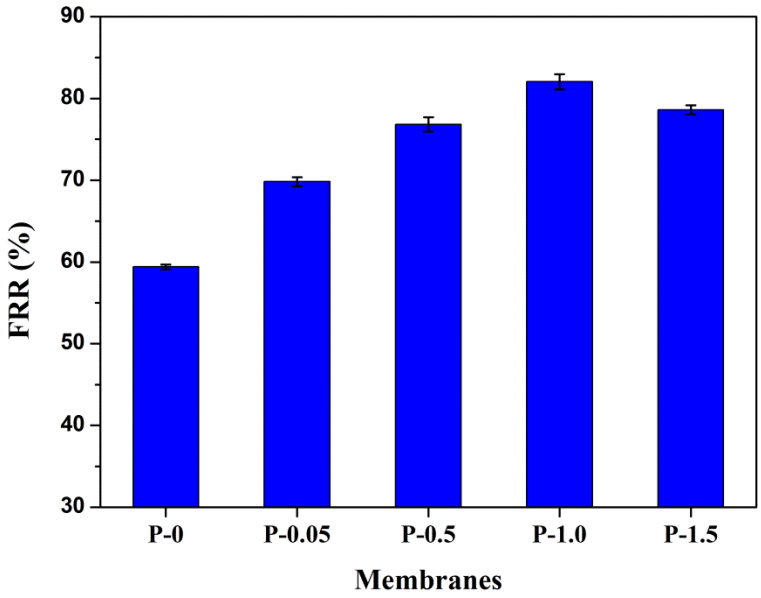

Fig. 11 % FRR values of the membranes

Membrane P-0 had least FRR value among all the membranes. The membranes showed increase in FRR value with PANI-TiO_2 content, indicating that addition of PANI-TiO_2 enhance the fouling resistance of membranes. As the hydrophilicity of the membranes increased with PANI-TiO_2 content, it weakened the interaction between membrane surface and the protein molecules. Thus the adsorbed BSA molecules on the membrane surface were easily removed by simple

washing resulting in high flux recovery ratio. The membrane P-1.5 showed little decrease in FRR value. This may be due to the decrease in hydrophilicity as observed by contact angle measurement.

The AFM results further confirmed that, addition of PANI-TiO_2 nanocomposite into the membranes improved the antifouling nature of membranes. It is well known that, lower the surface roughness of the membranes, better is the antifouling ability. From Fig. 5 and Table 2 it can be seen that membrane P-0 with no PANI-TiO_2 content was rough and surface roughness was reduced for P-0.5 and P-1.0 membranes. This decrease in surface roughness increased the antifouling nature of the membranes since the foulants are more likely to adsorb on course surfaces than smooth surface.[28]

3.2.8. Heavy Metal Ion Rejection

The heavy metal ion rejection by the membrane for metal ions Pb^{2+} and Cd^{2+} was studied by UF and PEUF process. Among the prepared membranes, the well performed membrane M-1.0 which possessed highest hydrophilicity, better permeability, highest FRR value was selected for the heavy metal ion rejection studies. Fig. 12 displays the % Rejection by the membrane during PEUF and UF process for heavy metal ions Pb^{2+} and Cd^{2+} respectively. The membrane exhibited 83.75% rejection for Pb^{2+} ions and 73.41% rejection for Cd^{2+} ions during PEUF. The % Rejection was higher for Pb than Cd this is because Pb^{2+}-PEI complex was larger in size than Cd^{2+}-PEI complex. The % rejection for Pb^{2+} and Cd^{2+} during UF was 68% and 53.78% respectively. The rejection of metal ions during UF process is due to the adsorption of metal ion on the membrane surface. Fig. 13 shows the elemental mapping of Pb and Cd adsorbed on the membranes. The main adsorption sites for metal ions were the nitrogen atoms of PANI of PANI-TiO_2 nanocomposite.[29] The unpaired electrons of the amine group of PANI can create co-ordinate bond with metal ions resulting in the adsorption of metal ions on the membrane surface.[30] The membranes showed higher % of rejection during PEUF process than UF process. This is because the metal ion-PEI complex has greater size than the membrane pore size. Hence the complexed metal ions are retained in the feed solution. During the UF process, most of the metal ions would easily pass through the membrane, as the pore size of the membrane is much higher than that of the metal ions. Only the metal ions adsorbed on to the membrane surface would contribute to the % rejection.

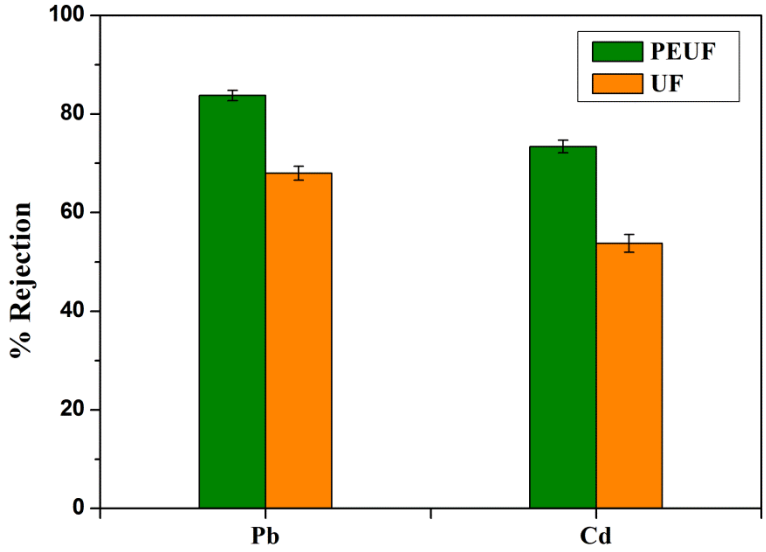

Fig. 12 Heavy metal ion rejection by the membranes

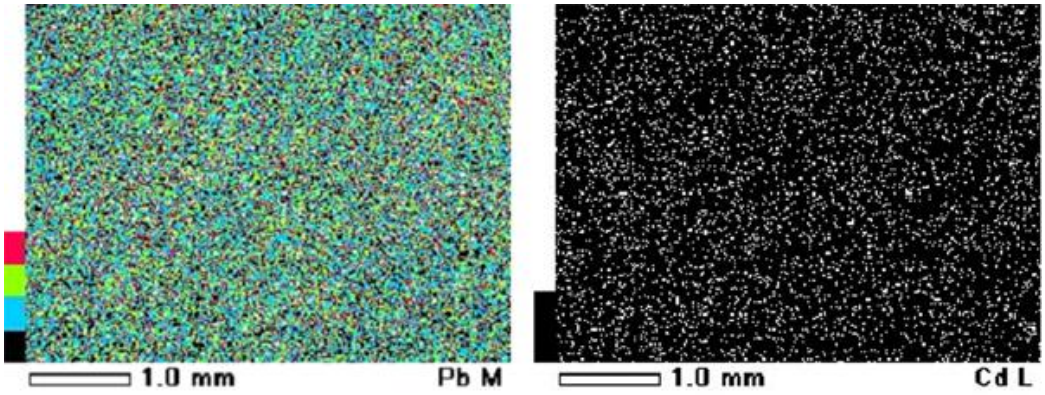

Fig. 13 Adsorption of Pb and Cd on the membranes

4. Conclusions

The performance of the polysulfone membranes can be improved by using PANI-TiO_2 nanocomposite as a hydrophilic additive. The properties of the membranes such as hydrophilicity, permeability, water uptake, porosity, antifouling nature enhanced with the addition of PANI-TiO_2 nanocomposite. The nanocomposite membranes also showed good rejection for Pb^{2+} and Cd^{2+} ions by PEUF process. Taking into account the contact angle, PWF ,

%FRR value, it is found that the properties of the membranes improved when the addition of PANI-TiO_2 nanocomposite was increased up to 1.0 wt %. When the concentration of the PANI-TiO_2 nanocomposite in the membranes was further increased to 1.5 wt %, the membranes showed slight decrease in performance. The decrease in performance by the membranes may be due to the agglomeration of the nanocomposite at higher concentration leading to clogging to pores. Thus it can be concluded that 1.0 wt % of PANI-TiO_2 nanocomposite is the threshold content for the synthesized membranes, beyond which the membrane show a decrease in performance.

Acknowledgements AMI is thankful to Prof. Swapan Bhattacharya, Director, National Institute of Technology Karnataka, Surathkal, India for providing the research facilities. The authors also thank Prof K. Narayan Prabhu of Department of Metallurgical and Materials Engineering, NITK Surathkal, India for providing the contact angle measurement facility.

References

1. X. Yi, S. Yu, W. Shi, S. Wang, N. Sun, L. Jin and C. Ma, *Desalination*, 2013, **319**, 38-46.
2. H. Song, Y. Jo, S.-Y. Kim, J. Lee and C. Kim, *J. Membr. Sci.*, 2014, **466**, 173-182.
3. R. Kumar, A. M. Isloor, A. F. Ismail, S. A. Rashid and T. Matsuura, *RSC Advances*, 2013, **3**, 7855.
4. J. Zhang, Y. Zhang, Y. Chen, L. Du, B. Zhang, H. Zhang, J. Liu and K. Wang, *Ind. Eng. Chem. Res.*, 2012, **51**, 3081-3090.
5. V. Moghimifar, A. Raisi and A. Aroujalian, *J. Membr. Sci.*, 2014, **461**, 69-80.
6. G. Zhang, S. Lu, L. Zhang, Q. Meng, C. Shen and J. Zhang, *J. Membr. Sci.*, 2013, **436**, 163-173.
7. H. Wu, B. Tang and P. Wu, *J. Membr. Sci.*, 2014, **451**, 94-102.
8. B. Wang, C. Liu, Y. Yin, S. Yu, K. Chen, P. Liu and B. Liang, *Composites Science and Technology*, 2013, **86**, 89-100.
9. Y.-G. Han, T. Kusunose and T. Sekino, *Journal of Ceramic Processing Research*, 2009, **10**, 208-211.
10. Y. Li, Y. Yu, L. Wu and J. Zhi, *Appl. Surf. Sci.*, 2013, **273**, 135-143.
11. S. B. Teli, S. Molina, A. Sotto, E. G. a. Calvo and J. d. Abajob, *Ind. Eng. Chem. Res.*, 2013, **52**, 9470-9479.
12. P. Daraei, S. S. Madaeni, N. Ghaemi, E. Salehi, M. A. Khadivi, R. Moradian and B. Astinchap, *J. Membr. Sci.*, 2012, **415-416**, 250-259.
13. S. Zhao, Z. Wang, X. Wei, B. Zhao, J. Wang, S. Yang and S. Wang, *Ind. Eng. Chem. Res.*, 2012, **51**, 4661-4672.
14. S. Xie, M. Gan, L. Ma, Z. Li, J. Yan, H. Yin, X. Shen, F. Xu, J. Zheng and J. Zhang, *Electrochimica Acta*, 2014, **120**, 408-415.
15. A. Katoch, M. Burkhart, T. Hwang and S. S. Kim, *Chem. Eng. J. (Lausanne)*, 2012, **192**, 262-268.
16. R. Kumar, A. M. Isloor, A. Ismail, S. A. Rashid and A. A. Ahmed, *Desalination*, 2013, **316**, 76-84.
17. Z. Fan, Z. Wang, N. Sun, J. Wang and S. Wang, *J. Membr. Sci.*, 2008, **320**, 363-371.
18. X. Li, W. Chen, C. Bian, J. He, N. Xu and G. Xue, *Appl. Surf. Sci.*, 2003, **217**, 16-22.

19. B. G. Lokesh, K. S. V. K. Rao, K. M. Reddy, K. C. Rao and P. S. Rao, *Desalination*, 2008, **233**, 166-172.
20. R. Kumar, A. Ismail, M. Kassim and A. M. Isloor, *Desalination*, 2013, **317**, 108-115.
21. M. Padaki, A. M. Isloor, G. Belavadi and K. N. Prabhu, *Ind. Eng. Chem. Res.*, 2011, **50**, 6528-6534.
22. A. K. Nair, A. M. Isloor, R. Kumar and A. F. Ismail, *Desalination*, 2013, **322**, 69-75.
23. F. Cheng, S. M. Sajedin, S. M. Kelly, A. F. Lee and A. Kornherr, *Carbohydr. Polym.*, 2014, **114**, 246-252.
24. V. R. Pereira, A. M. Isloor, U. K. Bhat and A. F. Ismail, *Desalination*, 2014, **351**, 220-227.
25. S. Nasirian and H. Milani Moghaddam, *Int. J. Hydrogen Energy*, 2014, **39**, 630-642.
26. V. Vatanpour, S. S. Madaeni, L. Rajabi, S. Zinadini and A. A. Derakhshan, *J. Membr. Sci.*, 2012, **401-402**, 132-143.
27. S. Zhao, Z. Wang, X. Wei, B. Zhao, J. Wang, S. Yang and S. Wang, *J. Membr. Sci.*, 2011, **385-386**, 251-262.
28. A. Razmjou, J. Mansouri and V. Chen, *J. Membr. Sci.*, 2011, **378**, 73-84.
29. A. Eisazadeh, H. Eisazadeh and K. A. Kassim, *Synthetic Metals*, 2013, **171**, 56-61.
30. M. Min, L. Shen, G. Hong, M. Zhu, Y. Zhang, X. Wang, Y. Chen and B. S. Hsiao, *Chem. Eng. J. (Lausanne)*, 2012, **197**, 88-100.